The Cerebellum (2025) 24:99
https://doi.org/10.1007/s12311-025-01850-x

RESEARCH

Alterations in the Na^+/H^+ Exchanger NHE6 and Glutamate Transporters may Influence Purkinje Cell Fate in ARSACS

Louis-Charles Masson[1] · Atchaya S. Kanagasabai[1] · Brenda Toscano Márquez[2] · Julia Tourbina-Kolomiets[1] · Francois Charron[1] · Alanna J. Watt[2] · R. Anne McKinney[1]

Accepted: 25 April 2025 / Published online: 15 May 2025
© The Author(s) 2025

Abstract

Patterned cell death is a common feature of many neurodegenerative diseases. This is apparent in cerebellar Purkinje cells (PCs) in patients and mouse models of Autosomal-recessive spastic ataxia of Charlevoix-Saguenay (ARSACS). In ARSACS, PCs in the anterior cerebellar vermis are vulnerable to degeneration while those in the posterior vermis are resilient. As the mechanisms underpinning cerebellar pathophysiology in ARSACS are not fully understood, we chose to investigate two important regulatory pathways for cellular health in neurons: (1) the autophagy-lysosome pathway which is important for the trafficking of cargo essential for proper neuronal function, as well as (2) excitatory amino acid transporters (EAATs) that regulate extracellular glutamate levels. Using a mouse model of ARSACS (*Sacs*$^{-/-}$), we found a significant decrease in the Na^+/H^+ exchanger 6 (NHE6) in the PCs in the vulnerable anterior but not resilient posterior cerebellum. We looked at two EAATs that are highly expressed in the cerebellum: EAAT1 and EAAT4. Glial EAAT1 levels were significantly reduced in both anterior and posterior lobules, which could lead to excitotoxicity. However, the neuronal EAAT4 protein was elevated only in the resilient posterior PCs, likely counteracting the effects of reduced EAAT1 in posterior cerebellum. These results point to possible impairment in the endocytic pathway in the ARSACS cerebellum, and an elevation of EAAT4 glutamate transporters in the resilient posterior lobules of the cerebellar vermis that may contribute to neuroprotection.

Keywords Ataxia · Endosomes · pH · Purkinje cells · Glutamate transporters

Introduction

Autosomal-recessive spastic ataxia of Charlevoix-Saguenay (ARSACS) is a progressive neurodegenerative disorder, originally discovered in the Charlevoix-Saguenay-Lac-Saint-Jean region of Québec [1]. Although more than 200 different mutations have been discovered, ARSACS is most often caused by a deletion mutation in the *SACS* gene, which encodes the large 520 kDa chaperone protein sacsin [1–3]. ARSACS is typically an early-onset disorder which leads to a progressively worsening ataxia with locomotor dysfunction [4, 5]. Currently, only symptomatic treatments are available for ARSACS, and we have only a poor understanding of how loss of sacsin leads to cellular dysfunction that gives rise to ataxia.

A sacsin knockout mouse (*Sacs*$^{-/-}$) has been developed, which recapitulates key disease phenotypes, including prominent ataxia and a progressive loss of the main output neurons of the cerebellar cortex, Purkinje cells (PCs) [6–8]. Interestingly, in both human patients and mouse models of ARSACS, the loss of PCs occurs in a stereotyped manner [7, 9]: PCs of the anterior lobes of the cerebellar vermis are most vulnerable, while PCs of the posterior vermis appear largely spared from cell death [7, 10]. Similar patterned cell death has been observed in several different types of ataxias, including Christianson syndrome (CS) ataxia [11–18],

Louis-Charles Masson and Atchaya S. Kanagasabai contributed equally to this work and share first authorship.

✉ Alanna J. Watt
alanna.watt@mcgill.ca

✉ R. Anne McKinney
anne.mckinney@mcgill.ca

[1] Department of Pharmacology and Therapeutics, McGill University, Montreal, QC, Canada

[2] Department of Biology, McGill University, Montreal, QC, Canada

suggesting that shared mechanisms may contribute to cell death. However, the mechanism(s) mediating selective PC vulnerability and resilience have yet to be fully elucidated. Their discovery may lead to novel therapeutic strategies that could prove effective in multiple forms of ataxias.

Recently, impairments in endocytic function have been reported in ARSACS [19], highlighting the potential role of sacsin in endo-lysosomal protein transport [19, 20]. The involvement of the endocytic pathway in the development of ataxias and other neurodegenerative disorders has been increasingly appreciated in the last decade [21, 22]. Impaired function of the endocytic pathway can be caused by altered levels of the endosomal Na^+/H^+ exchanger 6 (NHE6) found on the membranes of early and recycling endosomes. NHE6 maintains the organellar luminal pH level necessary for the accurate trafficking and sorting of cargo, ensuring proper neuronal function [23–25]. Altered expression of NHE6 has been shown to cause deficits in intracellular cargo trafficking due to over-acidified organelles in the endocytic pathway, leading to neuronal degeneration [16, 26] and ataxia in both a mouse model of CS [17, 27, 28] and in Shaker rats [29]. Hence, we sought to investigate whether ARSACS PC vulnerability could be linked to reduced levels of NHE6 in PCs.

Important cargo transported in the endocytic pathway in the cerebellar cortex are the excitatory amino acid transporters EAATs [30, 31]. These EAATs are responsible for maintaining low extracellular glutamate levels and preventing neurotoxicity. In the cerebellar cortex, the two predominant EAATs are EAAT1 expressed by astrocytic cells, such as Bergmann glia cells (BGCs), and EAAT4, expressed by PCs [32–35]. Altered expression of glutamate transporters has previously been reported in patterned PC death in other forms of ataxia [36, 37]. Since elevated glutamate and impaired glutamate clearance have been shown to contribute to ARSACS pathophysiology [38], we wondered whether changes in EAATs expression were observed in *Sacs*$^{-/-}$ mice.

We investigated changes in protein levels of NHE6 in *Sacs*$^{-/-}$ and litter-matched WT mouse PCs in two representative lobules of the cerebellar vermis: vulnerable anterior lobule III and resilient posterior lobule IX. Both regions are thought to be predominantly involved in motor control [39, 40]. We found that NHE6 protein levels were significantly decreased in PCs in the anterior lobule III but unchanged in the PCs of posterior lobule IX at P90, when PC death in anterior lobules has begun. This suggests that trafficking of endo-lysosomal cargo may be impaired in the vulnerable anterior PCs. A significant decrease in glial EAAT1 was found in both vulnerable and resilient lobules, suggestive of dysregulation of glutamate clearance in *Sacs*$^{-/-}$ PCs compared to WT cells. However, we observed an elevation in neuronal EAAT4 levels exclusively in resilient posterior lobule IX in *Sacs*$^{-/-}$ mice. The elevation of EAAT4 in *Sacs*$^{-/-}$ in the posterior of the vermis suggests that EAAT4 elevation may compensate for EAAT1 reduction in the posterior cerebellar vermis and thus protect posterior PC cells from glutamate-induced cell death.

Methods

Transgenic Animals

ARSACS (*Sacs*$^{-/-}$) mice carrying a deletion of the *Sacs* gene were used as previously described [6, 41, 42]. Heterozygous *Sacs*$^{+/-}$ mice were bred to obtain litter-matched *Sacs*$^{-/-}$ and wildtype (WT) mice. Equal numbers of male and female mice were used in all experiments. Experiments were performed on postnatal day P90 (N=4 for WT and N=4 for *Sacs*$^{-/-}$ mice). Breeding and animal procedures were approved by the McGill University Animal Care Committee. All experiments were performed in accordance with the rules and regulations established by the Canadian Council on Animal Care.

Tissue Preparation and Immunohistochemistry

For brain tissue acquisition, WT and *Sacs*$^{-/-}$ mice were deeply anesthetized with 2,2,2-tribromoethanol (Avertin) via intraperitoneal injection, and perfused transcardially with ice-cold phosphate-buffered saline (PBS, 0.1 M, pH 7.4), followed by transcardial fixation perfusion using ice-cold 4% paraformaldehyde (PFA). Brains were then extracted, and immersion fixed overnight in 4% PFA at 4ºC, before being washed with 0.1 M phosphate buffer (PB) and transferred to 0.1 M PB containing 0.05% sodium azide for storage at 4ºC. Immunohistochemistry was performed on sagittal free-floating cerebellar slices of 100 µm thickness obtained using a 5100mz vibratome (Campden Instruments, Lafayette, IN, USA). Slices were incubated overnight in permeabilization solution (0.1 M PB, 1.5% heat-inactivated horse serum (HIHS), 0.4% triton X-100, pH 7.4), then incubated with primary antibody diluted in permeabilization solution for 3 days at 4ºC on a 60 rpm shaker. Slices were then washed with blocking buffer (0.1 M PB, 1.5% HIHS, pH 7.4), then incubated with secondary antibody diluted in blocking buffer for 2 h at room temperature on a 60 rpm shaker, then washed with 0.1 M PB and mounted on Superfrost plus microscope slides (Fisher Scientific, Pittsburg, PA, USA) using Dako fluorescent mounting medium (Agilent Technologies, Santa Clara, CA, USA).

Immunohistochemistry Staining

For PC analyses, cerebellar sagittal slices were stained with primary antibody mouse anti-calbindin (1:1000; CB300, Swant, Marly, Switzerland) and rabbit anti-NHE6 (1:500; in-house antibody kindly gifted by Dr. John Orlowski, McGill University, Canada), or rabbit anti-EAAT4 (1:500; kind gift from Dr. Jeffrey Rothstein, Johns Hopkins University, USA). These primary antibodies were then tagged to secondary antibodies Alexa Fluor-488 conjugated goat anti-mouse (1:250; Invitrogen, Waltham, MA, USA) and DyLight-650 conjugated goat anti-rabbit (1:250; Invitrogen). For EAAT analyses, cerebellar sagittal slices of 100 µm were stained with primary antibodies rat anti-glial fibrillary acidic protein (GFAP, 1:500; 13–0300, Invitrogen) and guinea pig anti-EAAT1 (1:250; 250−114, Synaptic Systems, Göttingen, Germany). These primary antibodies were then tagged to respective secondary antibodies Alexa Fluor-488 conjugated goat anti-rat (1:250; 11006, Invitrogen) and DyLight-650 conjugated goat anti-guinea pig (1:250; SA510097, Invitrogen).

Confocal Imaging

Confocal images were acquired using a Zeiss LSM800 confocal fluorescent microscope equipped with Zen blue software (Zeiss, Oberkochen, Germany). Microscope settings were kept constant during the imaging process for all conditions. For analyses of PC dendrites and BGC processes, images were acquired using a 40x oil objective with no digital zoom. For analyses of PC soma, images were acquired using a 40x oil objective with a 2x zoom. Confocal microscope images were deconvolved using Huygens Confocal Deconvolution Software Essential Version 21.10 (Scientific Volume Imaging BV, North Holland, Netherlands). Imaris 9.6 image analysis software (Oxford Instruments, Abingdon, United Kingdom) was used to create a surface of either the calbindin (PC) or GFAP (BGC) signal, and a masked channel was then created to analyze the fluorescence intensity of either NHE6, EAAT4, or EAAT1 inside PC dendrites, PC somata, or BGC processes. Fluorescence intensity is reported in arbitrary units (A.U.). For fluorescence intensity quantification, primary-only and secondary-only controls were performed, and the reported values are the result of control values subtracted from the raw values. The researcher quantifying the data was blinded to the genotype. All representative images are shown in pseudo-color.

Statistics

Comparisons were made using GraphPad Prism 8.0.1 software. Data was first tested for normality with the Shapiro-Wilk test, then analyzed using Student's t-test (independent or paired) for normally distributed data, or Mann-Whitney U or Wilcoxon Signed Rank test for non-normally distributed data. Bonferroni correction was applied to p values to account for multiple comparisons. Data are represented by a box showing the median (horizontal line within boxes), first and third quartiles (rectangles) and whiskers extending to the minimum and maximum values. Significance was determined as $*p<0.05$, $**p<0.01$, $***p<0.001$, and $p>0.05$ if no comparison is shown.

Results

Levels of Endosomal Na^+/H^+ Exchanger NHE6 are Reduced in the Vulnerable Anterior Lobule III PCs of *Sacs*$^{-/-}$ Mice

To determine whether NHE6 protein levels are altered in ARSACS, we investigated NHE6 protein levels in PCs in cerebellar sagittal slices from WT and *Sacs*$^{-/-}$ mice at P90, a timepoint when PC loss is known to occur [7]. Cerebellar slices were labeled for the PC marker calbindin and the endosomal NHE6. The mean fluorescence intensity of NHE6 was quantified inside PC calbindin somata and dendrites (Fig. 1A-I). We measured NHE6 intensity in PCs in both a vulnerable anterior lobule (lobule III) and a resilient posterior lobule (lobule IX), as patterned cell death has been reported to occur exclusively in anterior lobules at this age [7]. We detected a significant decrease in NHE6 levels in both the PC somata and dendrites in *Sacs*$^{-/-}$ mice compared to WT in anterior lobule III (anterior dendrites (Student's t-test): $p<0.0196$; anterior soma (Mann-Whitney): $p<0.001$; Fig. 1D-I), while no detectable changes in NHE6 levels were found in PC somata and dendrites of lobule IX, when comparing *Sacs*$^{-/-}$ mice to WT mice. This specific reduction of NHE6 in the anterior lobule could alter the normal transport of cargo required for cellular function and contribute to the anterior lobule vulnerability.

Decreased Expression of the Glial Glutamate Transporter EAAT1 in BGC Processes of *Sacs*$^{-/-}$ Mice

One function of glial cells in proper synaptic function is in glutamate clearance through the expression of glutamate transporters. The expression of the glial-expressed EAAT1 is particularly high in BGCs processes [36], which run vertically through the cerebellar molecular layer where they interact closely with PCs [43, 44]. To investigate the expression level of EAAT1 in ARSACS, we stained sagittal cerebellar slices with GFAP as a marker of BGCs, as well as EAAT1, and compared EAAT1 levels inside BGC processes

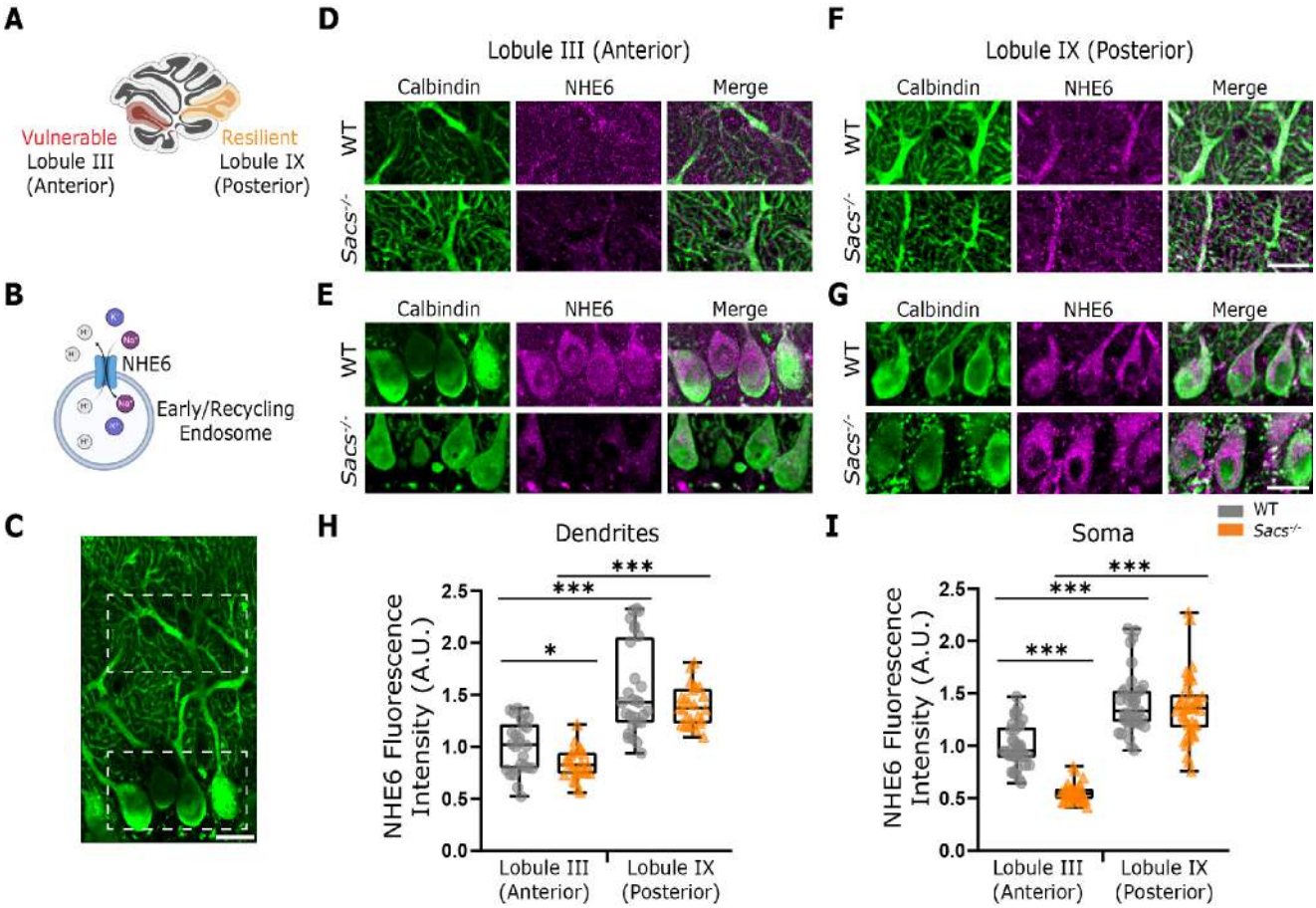

Fig. 1 Endosomal Na^+/H^+ exchanger isoform 6 (NHE6) levels are decreased in PCs of P90 *Sacs*$^{-/-}$ mice. (**A**) Illustrative image showing the region of interest in the cerebellar cortex where images were acquired, (**B**) Illustrative image showing the function of NHE6 in early and recycling endosomes. (**C**) Example of calbindin-stained PC dendrites and soma (green) (**D**, **E**) Representative images of anterior lobule III, from WT (top) and *Sacs*$^{-/-}$ (bottom) P90 mice, with PC dendrites (**D**) and soma (**E**) labeled with calbindin (green) and NHE6 (magenta). (**F**, **G**) Representative images of posterior lobule IX, from WT (top) and *Sacs*$^{-/-}$ (bottom) P90 mice, with PC dendrites (**F**) and soma (**G**) labeled with calbindin (green) and NHE6 (magenta). (**H**, **I**) NHE6 fluorescence intensity, reported in arbitrary units (A.U.), inside calbindin-labeled PC dendrites (**H**) and soma (**I**) was quantified in anterior lobule III (left) and posterior lobule IX (right), comparing WT (grey) and *Sacs*$^{-/-}$ (orange) mice. $N=4$ animals for WT, $N=4$ animals for *Sacs*$^{-/-}$ (**D**-**I**). For statistics, we used Student's t-test for normally distributed data and Mann-Whitney U test for non-normally distributed data and Wilcoxon Signed-Rank test was used to compare anterior with posterior; *$P<0.05$, **$P<0.01$, ***$P<0.001$, $P>0.05$ if no comparison is shown. Scale bar (**C**), (**F**), (**G**), 20 µm

in anterior and posterior lobules from WT and *Sacs*$^{-/-}$ mice (Fig. 2A-F). We found a significant decrease in EAAT1 expression in the BGC processes of *Sacs*$^{-/-}$ mice compared to WT in both anterior lobule III as well as posterior lobule IX (Mann-Whitney U test for all comparisons; anterior: $p<0.0001$; posterior: $p<0.0001$; Fig. 2F). A reduction in glutamate transporters could potentially lead to glutamate excitotoxicity, although, puzzlingly, this is observed in both vulnerable and resilient regions of the cerebellum.

Increased Levels of Neuronal Glutamate Transporter EAAT4 in Resilient PCs of *Sacs*$^{-/-}$ Mice

We wondered whether changes were observed in a second prominent glutamate transporter in the cerebellum, EAAT4, which normally displays a patterned expression with lower expression in the vulnerable anterior lobules, and higher expression in the resilient posterior lobules [36, 45]. We compared EAAT4 levels in WT and *Sacs*$^{-/-}$ mouse PC dendrites and somata at P90 (Fig. 3A-H), using the same cerebellar lobules to measure changes in vulnerable anterior (lobule III) and resilient posterior (lobule IX) cerebellum. We detected a significant increase in EAAT4 levels in PC somata of *Sacs*$^{-/-}$ mice compared to WT exclusively in the posterior lobule IX while no changes were observed in anterior lobule III (Mann-Whitney U test for anterior soma lobule III comparison, Student's t-test for posterior soma lobule IX and all dendrites comparisons; posterior somata $p=0.0148$, Fig. 3G-H). These findings suggest that an elevation of glutamate transporter EAAT4 in the posterior PC

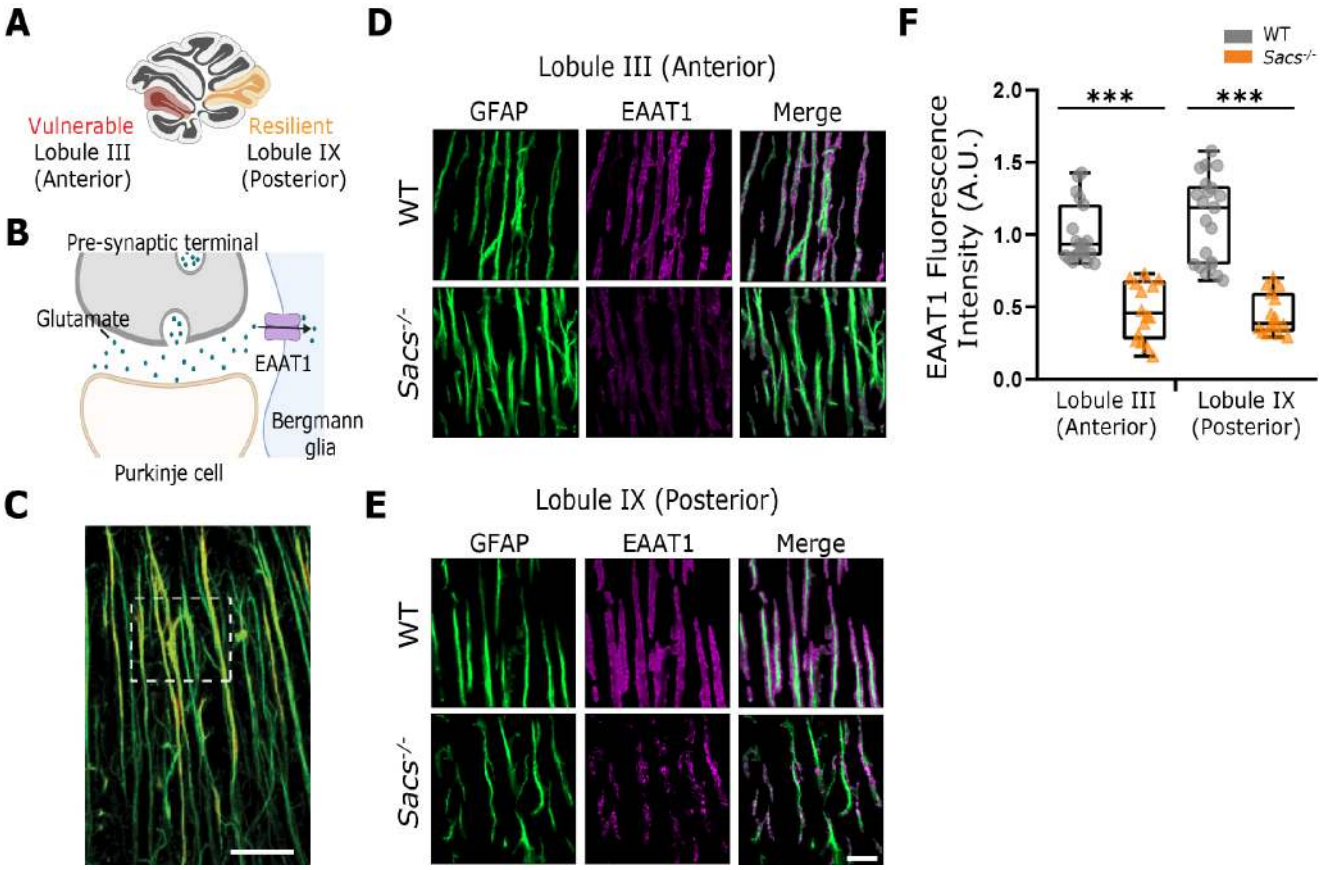

Fig. 2 Glial glutamate transporter EAAT1 shows decreased levels in BGC processes of P90 *Sacs*$^{-/-}$ mice. (**A**) Illustrative image showing the region of interest in the cerebellar cortex where images were acquired, (**B**) Illustrative image showing the function of EAAT1 in BGC processes. (**C**) Example of GFAP-stained BGC processes (green) (**D**) Representative images of anterior lobule III, from WT (top) and *Sacs*$^{-/-}$ (bottom) P90 mice, with BGC processes labeled with GFAP (green) and EAAT1 (magenta). (**E**) Representative images of posterior lobule IX, from WT (top) and *Sacs*$^{-/-}$ (bottom) P90 mice, with BGC processes labeled with GFAP (green) and EAAT1 (magenta). (**F**) EAAT1 fluorescence intensity, reported in arbitrary units (A.U.), inside GFAP-labeled BGC processes was quantified in anterior lobule III (left) and posterior lobule IX (right), comparing WT (grey) and *Sacs*$^{-/-}$ (orange) mice. $N=4$ animals for WT, $N=4$ animals for *Sacs*$^{-/-}$ (**D**-**F**). For statistics, Mann-Whitney U test was used to compare WT with *Sacs*$^{-/-}$ and Wilcoxon Signed-Rank test was used to compare anterior with posterior; $^{*}P<0.05$, $^{**}P<0.01$, $^{***}P<0.001$, $P>0.05$ if no comparison is shown. Scale bar (C, 20 µm, E, 10 µm)

cells could counteract the reduction observed in EAAT1 in the posterior cerebellum and protect these neurons from cell death, thereby conferring resilience.

Discussion

In this study, we determine whether changes in NHE6 or glutamate transporters are observed in a mouse model of ARSACS, which may contribute to patterned cell death in PCs (Fig. 4). We report that NHE6 is more highly expressed in posterior PCs in WT mice. However, in *Sacs*$^{-/-}$ mice, we observed significantly less NHE6 in the vulnerable anterior vermis while the posterior vermis had normal NHE6 levels. This correlates with the patterning of PC death that has been previously described in *Sacs*$^{-/-}$ mice [7, 42]. We also observed region-specific changes in glutamate transporters at the onset of cell death in the anterior lobules (P90): EAAT1 was downregulated in both anterior and posterior cerebellar vermis while EAAT4 was selectively upregulated in posterior cerebellar vermis, suggesting that EAAT4 upregulation may compensate for reduction in EAAT1 in the posterior cerebellar lobules that are spared, while the absence of compensatory changes in anterior lobules may result in elevated glutamate levels and cell death.

We postulate that at the onset of ataxia (P40), there would be a decrease in the level of EAAT1 in the anterior as we have previously reported a decrease in anterior Purkinje cell intrinsic firing in the *Sacs*$^{-/-}$ mouse model at this time point [6]. Decreases in intrinsic firing of PCs have been shown to occur when EAAT1 levels are reduced [36]. As EAAT1 levels progressively decrease over time, more and more pressure will be put on the cells to clear glutamate from the synaptic cleft without the aid of EAAT1. Once

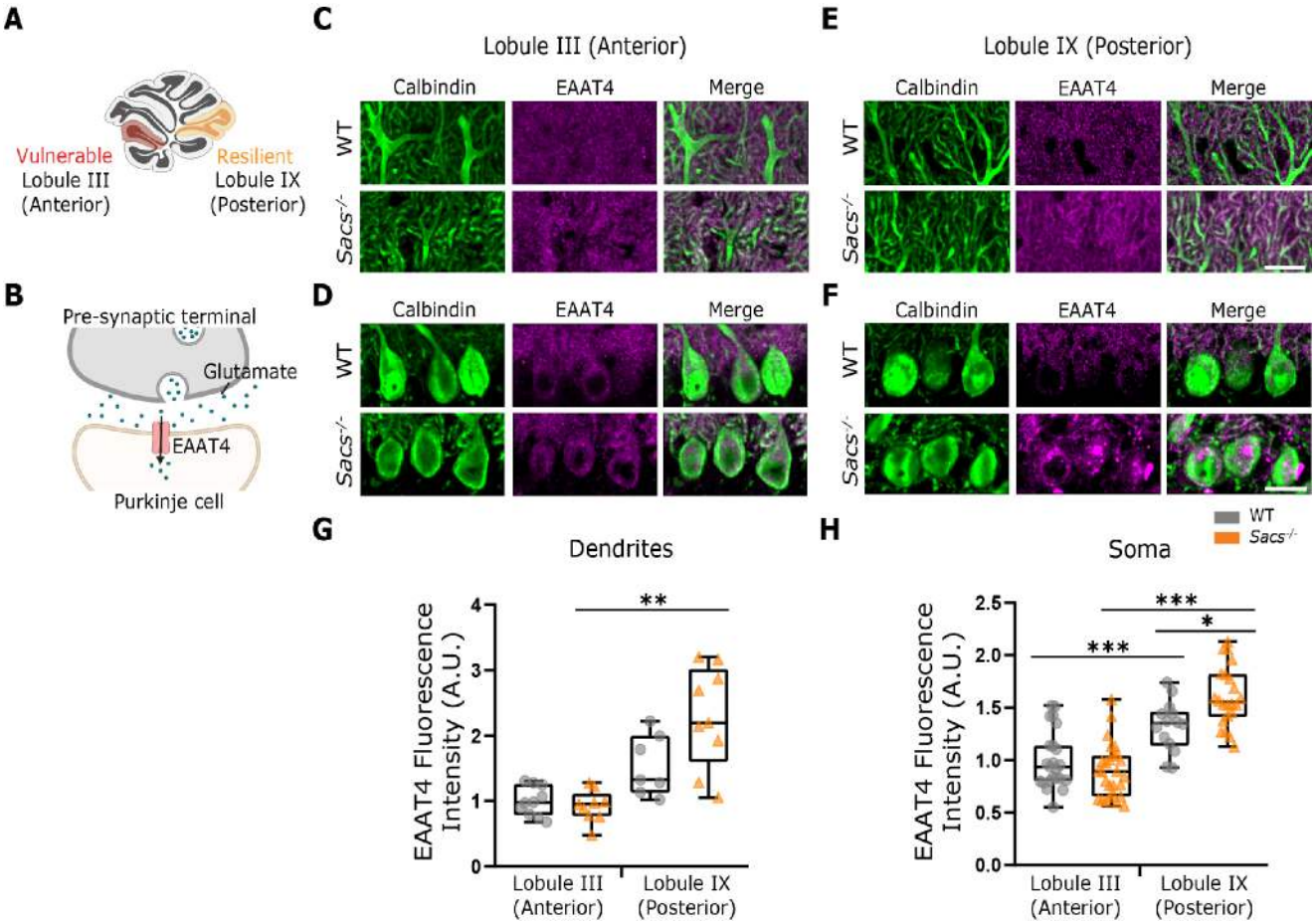

Fig. 3 Neuronal glutamate transporter EAAT4 shows increased levels in PCs of P90 *Sacs*$^{-/-}$ mice. (**A**) Illustrative image showing the region of interest in the cerebellar cortex where images were acquired, (**B**) Illustrative image showing the function of EAAT4 in PCs. (**C**, **D**) Representative images of anterior lobule III, from WT (top) and *Sacs*$^{-/-}$ (bottom) P90 mice, with PC dendrites (**C**) and soma (**D**) labeled with calbindin (green) and EAAT4 (magenta). (**E**, **F**) Representative images of posterior lobule IX, from WT (top) and *Sacs*$^{-/-}$ (bottom) P90 mice, with PC dendrites (**E**) and soma (**F**) labeled with calbindin (green) and EAAT4 (magenta). (**G**-**H**) EAAT4 fluorescence intensity, reported in arbitrary units (A.U.), inside calbindin-labeled PC dendrites (**G**) and soma (**H**) was quantified in anterior lobule III (left) and posterior lobule IX (right), comparing WT (grey) and *Sacs*$^{-/-}$ (orange) mice. $N=4$ animals for WT, $N=4$ animals for *Sacs*$^{-/-}$ (**C**-**H**). For statistics, Student's t-test for normally distributed data and Mann-Whitney U test for non-normally distributed data were used; $^{*}P<0.05$, $^{**}P<0.01$, $^{***}P<0.001$, $P>0.05$ if no comparison is shown. Scale bar (**E**-**F**), 20 μm

the levels of glutamate are increased to detrimental levels due to the reduction of glutamate clearance by EAAT1, PCs death would start in the anterior due to glutamate-mediated excitotoxicity. In fact, we did detect PCs death only in the anterior at P90 [7].

However, the posterior cells are able to remain alive by elevating their EAAT4 levels to compensate for the loss of EAAT1. Therefore, we do not believe that EAAT4 levels are increased in the posterior lobules prior to the onset of cell death in the anterior lobules, as there is no need for compensation at that stage. As the disease progresses, we speculate that the levels of EAAT4 will remain elevated to provide continuous compensation for the loss of EAAT1. In fact, we have previously shown that posterior PCs remain alive even as late as at P365, and elevated EAAT4 levels may be the mechanism through which they can do so [7]. Taken together, these results suggest that changes in endosomal exchanger NHE6 and in glutamate transporters EAAT1 and EAAT4 may contribute to patterned cell death in ARSACS.

To gain a better understanding of the effects of decreased NHE6 expression on neuronal circuitry, we can find clues from other disorders with endosomal deficits, such as CS, and Spinocerebellar ataxia type 6 (SCA6) [46]. CS is a mixed neurodevelopmental and neurodegenerative disorder characterized in part by ataxia and cerebellar atrophy [47–49]. Loss of function mutations in *SLC9A6*, the gene encoding NHE6 are the genetic cause of CS [17, 50]. Loss of NHE6 has been shown to lead to over-acidified endosomal compartments, resulting in trafficking deficits in the endocytic pathway [26, 51]. Although NHE6 expression is

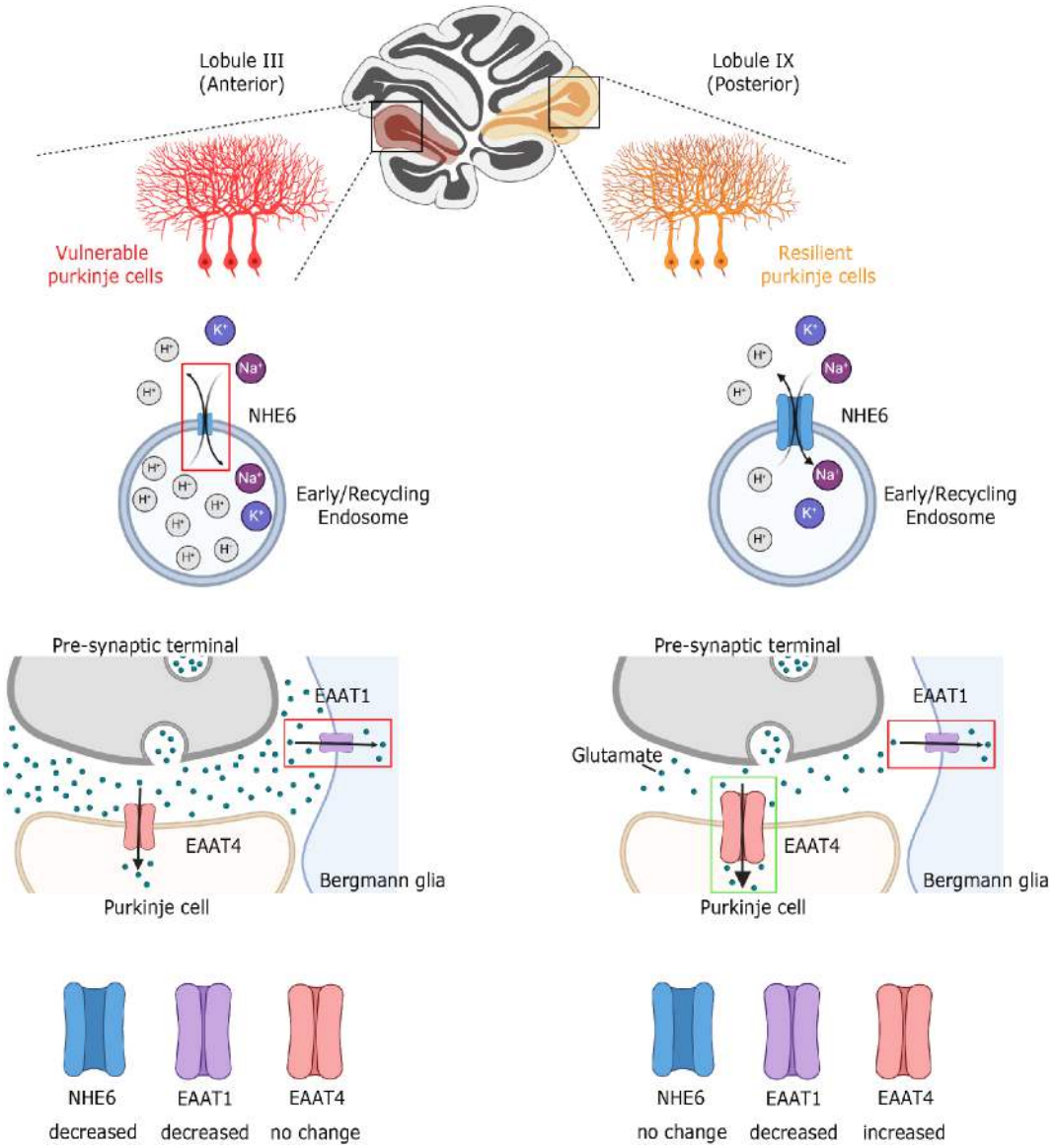

Fig. 4 NHE6 is lower only in the vulnerable anterior lobule of the ARSACS cerebellum, EAAT1 is reduced in both anterior and posterior lobules, but EAAT4 is elevated in the resilient posterior lobules of ARSACS cerebellum

limited to early and recycling endosomes, its ablation has profound effects on the overall function of the endocytic pathway. For example, NHE6 ablation is known to lead to defective endosome maturation, resulting in worsening lysosomal function over time [50]. One mechanism mediating the impaired lysosomal function in the absence of NHE6 is the over-acidified early and recycling endosomal lumen, resulting in mistrafficking of receptors [26] and premature activation of pH-dependent lysosomal degradation enzymes, such as cathepsin D [16, 52, 53]. These alterations downstream of NHE6 may contribute to pathophysiology in *Sacs*$^{-/-}$ mice, where a reduction of NHE6 in the anterior lobules impacts endocytic pathway in affected cells.

Cell death by excitotoxicity is a common pathological trigger of many neurodegenerative disorders, including some forms of cerebellar ataxia [37]. In fact, alterations in EAATs and glutamate-mediated excitotoxic cerebellar damage have been reported in several different forms of ataxias, and other neurological disorders [54–57]. It is currently unknown if EAAT1 levels have a sexually dimorphic expression in our *Sacs*$^{-/-}$ mice. Recently, following spinal cord injury, EAAT1 levels were found to be lower in males compared to female mice [58]. If such differences also exist in *Sacs*$^{-/-}$ mice, then an equivalent decrease in EAAT1 could have a larger effect on male mice, potentially decreasing glutamate clearance and increasing excitotoxicity compared to females. Cell death by excitotoxicity is caused by excessive glutamate

in the extracellular space and synaptic cleft that provokes a cascade of reactions inside neurons involving dysregulated Ca^{2+} homeostasis and glutamate-mediated neurotoxicity. A previous study in *Sacs*$^{-/-}$ mice found impaired Ca^{2+} homeostasis in cerebellar PCs [38] that could be partially restored by ceftriaxone, which is known to upregulate transcription of EAAT2/GLT-1 [38, 59]. Our findings of reduction in EAAT1 and region-specific upregulation of EAAT4 could at least in part suggest a means by which glutamate-mediated excitotoxicity may contribute to neuronal degeneration in ARSACS. Future studies are needed to understand how EAAT4 is upregulated in posterior lobule PCs, since this could be therapeutically relevant for treatment.

Acknowledgements We thank all past and present members of the McKinney and Watt labs for constructive and thoughtful feedback on the project. Imaging was performed at the McGill University Advanced BioImaging Facility (ABIF), and we thank ABIF staff members for their technical support. We are grateful for the animal care and training we received from the McGill Animal Resources Centre (CMARC), and particularly for the expert help of Tanya Koch.

Author Contributions RM and AW conceived and designed the manuscript, supervised the study. LCM, BT, ASK, JTK and FC performed the experiments and analyzed the data. RM and AW wrote the manuscript. LCM and ASK contributed equally as first author.

Funding Funding was provided by the Ataxia Charlevoix-Saguenay (ARSACS) Foundation Research Grant.

Data Availability No datasets were generated or analysed during the current study.

Declarations

Competing Interests The authors declare no competing interests.

Open Access This article is licensed under a Creative Commons Attribution-NonCommercial-NoDerivatives 4.0 International License, which permits any non-commercial use, sharing, distribution and reproduction in any medium or format, as long as you give appropriate credit to the original author(s) and the source, provide a link to the Creative Commons licence, and indicate if you modified the licensed material. You do not have permission under this licence to share adapted material derived from this article or parts of it. The images or other third party material in this article are included in the article's Creative Commons licence, unless indicated otherwise in a credit line to the material. If material is not included in the article's Creative Commons licence and your intended use is not permitted by statutory regulation or exceeds the permitted use, you will need to obtain permission directly from the copyright holder. To view a copy of this licence, visit http://creativecommons.org/licenses/by-nc-nd/4.0/.

References

1. Engert JC, et al. ARSACS, a spastic ataxia common in Northeastern Québec, is caused by mutations in a new gene encoding an 11.5-kb ORF. Nat Genet. 2000;24(2):120–5.
2. Bouchard J, et al. Autosomal recessive spastic ataxia of Charlevoix-Saguenay. Can J Neurol Sci. 1978;5(1):61–9.
3. Parfitt DA, et al. The ataxia protein Sacsin is a functional co-chaperone that protects against polyglutamine-expanded ataxin-1. Hum Mol Genet. 2009;18(9):1556–65.
4. Bagaria J, Bagyinszky E, An SSA. Genetics of autosomal recessive spastic Ataxia of Charlevoix-Saguenay (ARSACS) and role of Sacsin in neurodegeneration. Int J Mol Sci, 2022. 23(1).
5. Vermeer S, et al. ARSACS in the Dutch population: a frequent cause of early-onset cerebellar ataxia. Neurogenetics. 2008;9(3):207–14.
6. Ady V, et al. Altered synaptic and firing properties of cerebellar purkinje cells in a mouse model of ARSACS. J Physiol. 2018;596(17):4253–67.
7. Toscano Márquez B, et al. Molecular identity and location influence purkinje cell vulnerability in Autosomal-Recessive spastic Ataxia of Charlevoix-Saguenay mice. Front Cell Neurosci. 2021;15:707857.
8. Artero Castro A, et al. Short review: investigating ARSACS: models for Understanding cerebellar degeneration. Neuropathol Appl Neurobiol. 2019;45(6):531–7.
9. Sarna JR, Hawkes R. Patterned purkinje cell death in the cerebellum. Prog Neurobiol. 2003;70(6):473–507.
10. Lessard I, et al. Natural history of autosomal recessive spastic Ataxia of Charlevoix-Saguenay: a 4-Year longitudinal study. Cerebellum. 2024;23(2):489–501.
11. Prasad H, Rao R. The Na+/H+exchanger NHE6 modulates endosomal pH to control processing of amyloid precursor protein in a cell culture model of alzheimer disease. J Biol Chem. 2015;290(9):5311–27.
12. Fernandez MA, et al. Loss of endosomal exchanger NHE6 leads to pathological changes in Tau in human neurons. Stem Cell Rep. 2022;17(9):2111–26.
13. Pohlkamp T, et al. NHE6 depletion corrects ApoE4-mediated synaptic impairments and reduces amyloid plaque load. eLife. 2021;10:e72034.
14. Meda SA, et al. A large scale multivariate parallel ICA method reveals novel imaging–genetic relationships for Alzheimer's disease in the ADNI cohort. NeuroImage. 2012;60(3):1608–21.
15. Prasad H, Rao R. Endosomal Acid-Base homeostasis in neurodegenerative diseases. Rev Physiol Biochem Pharmacol. 2023;185:195–231.
16. Pescosolido MF, et al. Loss of Christianson syndrome Na(+)/H(+) exchanger 6 (NHE6) causes abnormal endosome maturation and trafficking underlying lysosome dysfunction in neurons. J Neurosci. 2021;41(44):9235–56.
17. Gilfillan GD, et al. SLC9A6 mutations cause X-linked mental retardation, microcephaly, epilepsy, and ataxia, a phenotype mimicking Angelman syndrome. Am J Hum Genet. 2008;82(4):1003–10.
18. Clark HB, et al. Purkinje cell expression of a mutant allele of SCA1 in Transgenic mice leads to disparate effects on motor behaviors, followed by a progressive cerebellar dysfunction and histological alterations. J Neurosci. 1997;17(19):7385–95.
19. Francis V, et al. The ARSACS disease protein Sacsin controls lysosomal positioning and reformation by regulating microtubule dynamics. J Biol Chem. 2022;298(9):102320.
20. Duncan EJ, et al. Altered organization of the intermediate filament cytoskeleton and relocalization of proteostasis modulators in cells lacking the ataxia protein Sacsin. Hum Mol Genet. 2017;26(16):3130–43.
21. Hivare P, et al. Endocytic pathways of pathogenic protein aggregates in neurodegenerative diseases. Traffic. 2023;10:434–52.
22. Schreij AM, Fon EA, McPherson PS. Endocytic membrane trafficking and neurodegenerative disease. Cell Mol Life Sci. 2016;73(8):1529–45.

23. Flessner R, Orlowski J. Na+/H+Exchangers. Encyclopedia of molecular Pharmacology. Cham: Springer International Publishing; 2021. pp. 1047–62. S. Offermanns and W. Rosenthal, Editors.
24. Kondapalli KC, Prasad H, Rao R. An inside job: how endosomal Na(+)/H(+) exchangers link to autism and neurological disease. Front Cell Neurosci. 2014;8:172.
25. Elkin SR, Lakoduk AM, Schmid SL. Endocytic pathways and endosomal trafficking: a primer. Wien Med Wochenschr. 2016;166(7–8):196–204.
26. Gao AYL, et al. A Christianson syndrome-linked deletion mutation (Δ287ES288) in SLC9A6 impairs hippocampal neuronal plasticity. Neurobiol Dis. 2019;130:104490.
27. Xu M et al. Mixed neurodevelopmental and neurodegenerative pathology in Nhe6-Null mouse model of Christianson syndrome. eNeuro, 2017;4(6).
28. Ouyang Q, et al. Christianson syndrome protein NHE6 modulates TrkB endosomal signaling required for neuronal circuit development. Neuron. 2013;80(1):97–112.
29. Figueroa KP, et al. Slc9a6 mutation causes purkinje cell loss and ataxia in the shaker rat. Hum Mol Genet. 2023;32(10):1647–59.
30. Malik AR, Willnow TE. Excitatory amino acid transporters in physiology and disorders of the central nervous system. Int J Mol Sci, 2019;20(22).
31. Iovino L, et al. Trafficking of the glutamate transporter is impaired in LRRK2-related Parkinson's disease. Acta Neuropathol. 2022;144(1):81–106.
32. Zhou Y, Danbolt NC. Glutamate as a neurotransmitter in the healthy brain. J Neural Transm (Vienna). 2014;121(8):799–817.
33. Furuta A et al. Cellular and synaptic localization of the neuronal glutamate transporters excitatory amino acid transporter 3 and 4. 1997;81(4):1031–42.
34. Rothstein JD, et al. Localization Neuronal Glial Glutamate Transporters. 1994;13(3):713–25.
35. Ozawa S. [Role of glutamate transporters in excitatory synapses in cerebellar purkinje cells]. Brain Nerve. 2007;59(7):669–76.
36. Perkins EM, et al. Loss of cerebellar glutamate transporters EAAT4 and GLAST differentially affects the spontaneous firing pattern and survival of purkinje cells. Hum Mol Genet. 2018;27(15):2614–27.
37. Slemmer JE, De Zeeuw CI, Weber JT. Don't get too excited: mechanisms of glutamate-mediated purkinje cell death. Prog Brain Res. 2005;148:367–90.
38. Del Bondio A et al. Restoring calcium homeostasis in purkinje cells arrests neurodegeneration and neuroinflammation in the ARSACS mouse model. JCI Insight, 2023;8(12).
39. Lin Y-C et al. Relatsh between Zebrin Expression Cerebellar Functions: Insights Neuroimaging Stud. 2020;11.
40. Stoodley CJ, Valera EM, Schmahmann JD. Functional topography of the cerebellum for motor and cognitive tasks: an fMRI study. NeuroImage. 2012;59(2):1560–70.
41. Girard M, et al. Mitochondrial dysfunction and purkinje cell loss in autosomal recessive spastic ataxia of Charlevoix-Saguenay (ARSACS). Proc Natl Acad Sci. 2012;109(5):1661–6.
42. Lariviere R, et al. Sacs knockout mice present pathophysiological defects underlying autosomal recessive spastic ataxia of Charlevoix-Saguenay. Hum Mol Genet. 2015;24(3):727–39.
43. Leung AW, Li JYH. The molecular pathway regulating Bergmann glia and folia generation in the cerebellum. Cerebellum. 2018;17(1):42–8.
44. Bordey A, Sontheimer H. Modulation of glutamatergic transmission by Bergmann glial cells in rat cerebellum. Situ. 2003;89(2):979–88.
45. Cerminara NL, et al. Redefining the cerebellar cortex as an assembly of non-uniform purkinje cell microcircuits. Nat Rev Neurosci. 2015;16(2):79–93.
46. Cook AA et al. Endosomal dysfunction contributes to cerebellar deficits in spinocerebellar ataxia type 6. Elife, 2023;12.
47. Bosemani T, et al. Christianson syndrome: spectrum of neuroimaging findings. Neuropediatrics. 2014;45(4):247–51.
48. Schroer RJ, et al. Natural history of Christianson syndrome. Am J Med Genet A. 2010;152a(11):2775–83.
49. Morrow EM, Pescosolido MF et al. Christianson Syndrome, in GeneReviews(®), M.P. Adam, Editors. 1993, University of Washington, Seattle Copyright © 1993–2023, University of Washington, Seattle. GeneReviews is a registered trademark of the University of Washington, Seattle. All rights reserved.: Seattle (WA).
50. Pescosolido MF, et al. Genetic and phenotypic diversity of NHE6 mutations in Christianson syndrome. Ann Neurol. 2014;76(4):581–93.
51. Ilie A, et al. A Christianson syndrome-linked deletion mutation (Δ(287)ES(288)) in SLC9A6 disrupts recycling endosomal function and elicits neurodegeneration and cell death. Mol Neurodegener. 2016;11(1):63.
52. Vidoni C, et al. The role of cathepsin D in the pathogenesis of human neurodegenerative disorders. Med Res Rev. 2016;36(5):845–70.
53. Schwagerl AL, et al. Elevated levels of the endosomal-lysosomal proteinase cathepsin D in cerebrospinal fluid in alzheimer disease. J Neurochem. 1995;64(1):443–6.
54. Shuvaev AN, et al. Chronic optogenetic stimulation of Bergman glia leads to dysfunction of EAAT1 and purkinje cell death, mimicking the events caused by expression of pathogenic ataxin-1. Neurobiol Dis. 2021;154:105340.
55. Wu Q et al. Ataxia-linked SLC1A3 mutations alter EAAT1 chloride channel activity and glial regulation of CNS function. J Clin Invest, 2022;132(7).
56. Colucci E, et al. Mutation in glutamate transporter homologue GltTk provides insights into pathologic mechanism of episodic ataxia 6. Nat Commun. 2023;14(1):1799.
57. Gorostiola González M, et al. Molecular insights into disease-associated glutamate transporter (EAAT1 / SLC1A3) variants using in Silico and in vitro approaches. Front Mol Biosci. 2023;10:1286673.
58. Colón-Mercado JM, et al. The sexually dimorphic expression of glutamate transporters and their implication in pain after spinal cord injury. Neural Regen Res. 2025;20(11):3317–29.
59. Fan S, et al. Ceftriaxone improves cognitive function and upregulates GLT-1-Related Glutamate-Glutamine cycle in APP/PS1 mice. J Alzheimers Dis. 2018;66(4):1731–43.

Publisher's Note Springer Nature remains neutral with regard to jurisdictional claims in published maps and institutional affiliations.